A Discussion on the Coupling Effects in Conductor-Backed Coplanar Waveguide MIC's with Lateral Sidewalls

Mark A. Magerko, Lu Fan and Kai Chang

Dept. of Electrical Engineering, Texas A&M University
College Station, TX, USA 77843-3128

Abstract --- Conductor-backed coplanar waveguide (CBCPW) with lateral sidewalls can support rectangular waveguide modes that couple with the dominant mode and can produce several undesirable results. These modes can be cutoff by reducing the lateral dimensions of the structure but for higher frequency operation the available circuit surface area is severely limited. The CBCPW is analyzed with a two-dimensional spectral domain method to demonstrate these coupling effects and the results provide insight to the characteristics of finite length structures.

I. INTRODUCTION

Coplanar waveguides with conductor backing to support the structure (see Fig.1) offer an attractive alternative to microstrip as a transmission media for MIC's. Lateral sidewalls (2b of Fig. 1) are incorporated to connect the top and bottom conductor ground planes without the use of via holes. The sidewalls could also represent the boundary effects of the CBCPW in a package. This structure resembles a rectangular waveguide with two aperture slots to guide the electromagnetic energy. Rectangular waveguides modes operating above their cutoff frequency are excited at circuit discontinuities (i.e. coaxial connector feed) and will propagate and couple with the dominant zero-cutoff CBCPW mode. The presence of these modes can cause the CBCPW mode field distribution to spread across the entire waveguide width instead of being confined to the slot regions [1] and modify its propagation characteristics. According to coupled-mode theory [2], power can be exchanged between modes as they propagate and is dependent on the transmission line length. Energy outside the slot cross section of the CBCPW (W+2S of Fig. 1) will not be detected by the coaxial connector and will resonate in the finite length cavity structure (the connector housing blocks complete the cavity at z=0, z=*L* of Fig. 1). The larger this energy is, the stronger the resonance. The type of discontinuity will also affect the coupling.

To completely avoid the coupling problems, the CBCPW dimensions can be chosen to cutoff the waveguide modes. This is most easily achieved by reducing the lateral sidewall separation [3]. However, to operate at higher frequencies, the narrow wall separation drastically reduces the available MIC surface area [4]. For a practical circuit the lateral walls must be extended allowing the rectangular waveguide modes to propagate. Multi-mode operation will occur in GaAs CBCPW MMIC's with a lateral dimension of 1mm operating above approximately 40 GHz. The spectral domain method (SDM) predicts the coupling effects and propagation of the modes of the CBCPW. The analysis includes the characteristics associated with the mode impedances, coupling coefficients, field plots, and field spreading of the dominant CBCPW mode. For multi-mode operation, the line length must accompany the procedure and we are presently investigating this problem. Experimental data demonstrates the coupling effects within CBCPW.

II. ANALYSIS

The procedure assumes that the CBCPW is symmetric, lossless and infinite in length, and the top ground conductors extend to the substrate edge and are connected to the conductor backing via the lateral ideal PEC sidewalls. The waveguide in Fig. 1 is modeled as a shielded structure for the SDM with a large separation between the top conductors and the top wall. An ideal magnetic wall exists at the center plane of the structure at x=0 (see Fig. 1) since this is the excitation of the dominant CBCPW mode [5]. The CBCPW is described in a multi-layer configuration since this structure can increase the waveguide mode cutoff frequencies and reduce the coupling as shown experimentally [6]. The SDM predicts the mode propagation characteristics applying the hybrid field modes TMy_{mn} and TEy_{mn}. The magnetic wall excitation requires n=1,3,5,... for each case above and will only support modes with even E_y and E_z and odd E_x field distributions about the center plane. The slot fields for the CBCPW mode were expanded using sine and cosine basis

OF2

functions with edge condition terms [5]. The identical basis functions were used for the waveguide modes since the same field constraints apply and the fields should fringe across the slots due to the conductor potential difference. Dispersion curves for the first few higher order waveguide modes in air suspended CBCPW have been shown in [7] but the modes were not identified and coupling effects were not discussed. The characteristic impedance of the modes was calculated using a voltage-power definition [5] since the mode field distribution extends across the entire waveguide width. The coupling coefficients (field overlap integrals) between the waveguide and CBCPW modes are utilized in the coupled-mode theory [2] and are evaluated using an expression from [8]. The waveguide modes cutoff frequencies can be approximated ignoring the aperture slots using expressions from [9]. The presence of the slots in the CBCPW perturbs the waveguide mode fields and with air above the structure, the waveguide mode cutoff frequencies are increased proportionally to the slot cross section area.

III. NUMERICAL RESULTS

The results presented are based on the following CBCPW structure ε_{r2}=2.33 h_2=0.381 mm, ε_{r1}=10.8 h_1=1.27 mm, W=2S=0.635 mm, 2b=38 mm. The dispersion curves calculated by the SDM for CBCPW and waveguide modes (TMy_{01}, TMy_{03},..., $TMy_{0,17}$, $TMy_{0,19}$) are shown in Fig. 2. Above 32.5 GHz the TMy_{1n} and TEy_{0n} modes can propagate but are not included as this would clutter the graph. A longitudinal phase velocity match condition between the CBCPW and waveguide modes does not occur but rather regions of strong coupling exist. The cross sectional mode field patterns are exhibited in Fig. 3. Fig. 4 depicts the field plots for the CBCPW and first few waveguide modes. The field components have been normalized to their maximum values. The field orientations of the waveguide modes are reversed for frequencies before and after the region of strong coupling with CBCPW mode (i.e. TMy_{01} field pattern is in positive y-direction below 7 GHz). The coupling effects due to the lateral sidewalls result in the field spreading of the CBCPW mode and are depicted in Fig. 5. From Fig. 4 the CBCPW mode is still confined to the slot regions, but this is not the case at higher frequencies. The CBCPW mode is shown at frequencies before the strong coupling regions (see Fig. 2) with TMy_{05}, TMy_{07}, TMy_{09} modes. The field spreading appears to become much worse after the coupling to the TMy_{05} mode. Fig. 6 calculates the impedances for the modes indicated in Fig. 2. The impedance of the waveguide modes away from the region of strong coupling should be small since their fields have a large amplitude and are extended across the entire waveguide width which translates into a much higher power flow. The impedance of the CBCPW mode should decrease with frequency for this case as its field distribution resembles that of a waveguide mode from the coupling effects. The coupling coefficients between the waveguide modes to the CBCPW mode are shown in Fig. 7 and the peak values corresponds to the impedance intersection points of Fig. 6.

IV. EXPERIMENTAL RESULTS

Fig. 8 depicts S-parameter data of CBCPW lines on a test fixture using Duroid™ substrates with an HP8510 using 401 frequency points. The bottom conductor is connected to the top ground planes by copper tape that folds around the sides of the boards. CASES A-B and C-D show the coupling dependency as a function of length. For CASE C the coupling effects with the waveguide modes is weak (as the SDM predicts) and the CBCPW mode is tightly bound to the slots across the frequency band. Therefore, energy is coupled to the waveguide modes at the coaxial feed or by the CBCPW mode over the waveguide length. By reducing the cavity (transmission line) length, the resonances should be shifted upward in frequency and modify the Q somewhat. This statement is verified for the lower half of the band for CASE D but the upper band resonances have effectively disappeared. The resonance at 23 GHz (beginning of the upper band resonances) of CASE C could correspond approximately to either $TMy_{0,1,12}$, $TMy_{0,3,11}$,or $TMy_{0,5,8}$ modes for an ideal multi-layer cavity at L=38 mm. For L=25.4 mm the resonant frequencies for these modes are 32.8, 31.9, 28.7 GHz respectively which are all within the measurement band. The broadband absorber of CASES E and F reduces the resonances associated with the waveguide modes. CASE F shows the minimal effect of the copper tape in our data.

V. CONCLUSION

The undesirable coupling associated with propagating waveguide modes in practical MIC's have been identified, demonstrated numerically, and shown experimentally. The coupling problems will occur in CBCPW MMIC's in the millimeter-wave frequency range. These effects have been described via a two-dimensional SDM and the results provide insight to the characteristics of finite length (three-dimensional) structures.

VI. ACKNOWLEDGMENTS

This work was supported by a fellowship to M. Magerko by the U.S. Department of Education - Areas of National Need Program.

VII. REFERENCES

[1] G. Leuzzi, A. Silbermann and R. Sorrentio, "Mode propagation in laterally bounded conductor-backed coplanar waveguides," in *1983 IEEE MTT-S Int. Microwave Symp. Dig.*, pp. 393-395.

[2] W.M. Louisell, *Coupled Mode and Parametric Electronics*, New York: Wiley, pp. 18-34, 1960.

[3] R.W. Jackson, "Mode conversion at discontinuities in finite-width conductor-backed coplanar waveguide," *IEEE Trans. Microwave Theory Tech.*, vol. MTT-37, no. 10, pp. 1582-1589.

[4] R.N. Simmons, G.E. Ponchak, K.S. Martzaklis and R.R. Romanofsky, "Channelized CPW: discontinuities, junctions, and propagation characteristics," in *1989 IEEE MTT-S Int. Microwave Symp. Dig.*, pp. 915-918.

[5] T. Itoh, *Numerical Techniques for Microwave and Millimeter-Wave Passive Structures*, New York: Wiley, pp. 324-380, 1989.

[6] M.A. Magerko, L. Fan and K. Chang, "Multiple dielectric structures to eliminate moding problems in CBCPW MIC's," *IEEE Microwave Guided Wave Lett.*, vol. 2, no. 6, pp. 257-259, 1992.

[7] Y. Fujiki, M. Suzuki and Y. Hayashi, "Higher-order modes in coplanar-type transmission lines," *Electronics and Communications in Japan*, vol. 58-B, no. 2, pp. 74-81, 1975.

[8] L. Chou, R. Rojas and P. Pathak, "A WH/GSMT based full-wave analysis of the power leakage from CBCPW," in *1992 IEEE MTT-S Int. Microwave Symp. Dig.*, pp. 219-222.

[9] R.F. Harrington, *Time-Harmonic Electromagnetic Fields*, New York: McGraw-Hill, pp. 158-160, 1961.

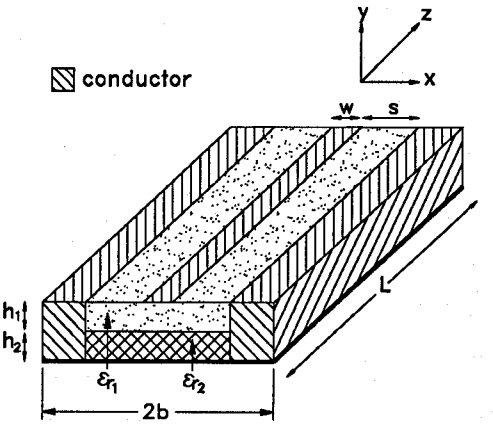

Fig. 1 Physical CBCPW structure with the coordinate system located at the bottom ground conductor.

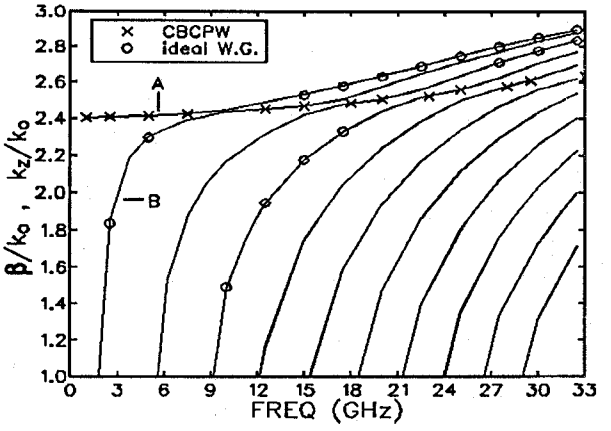

Fig. 2 Dispersion curves for CBCPW and waveguide modes. Ideal W.G. refers to a two-layer rectangular waveguide propagation constants without slots.

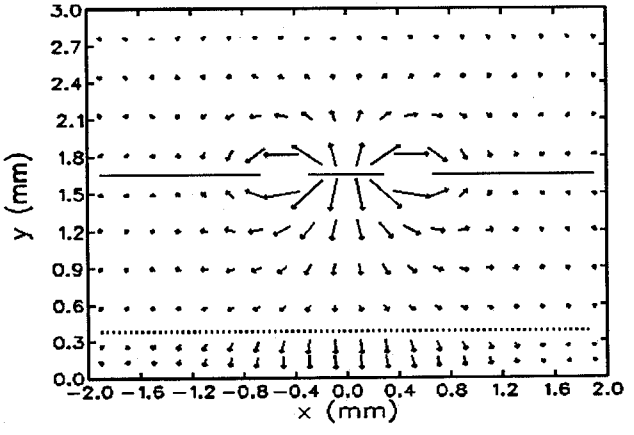

(a)

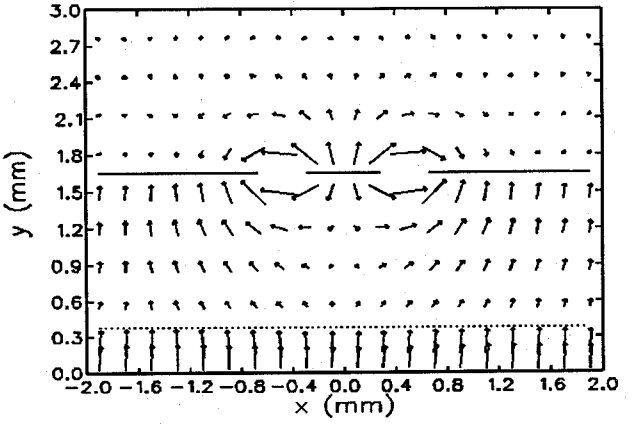

(b)

Fig. 3 Cross sectional vector field plots at 20 GHz for a) CBCPW mode, b) TMy_{05} mode.

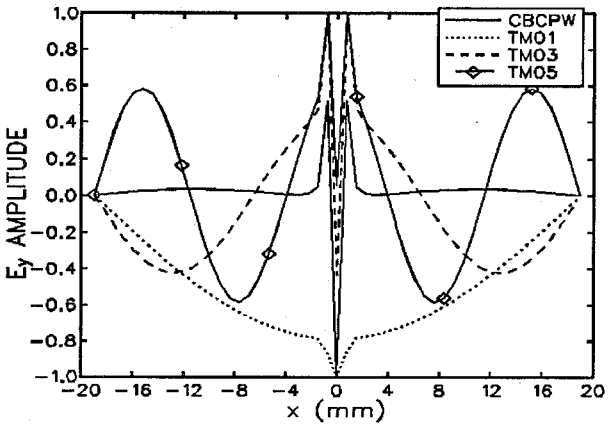

Fig. 4 Plots of CBCPW and waveguide modes at 15 GHz and y=h1+h2-0.01 mm.

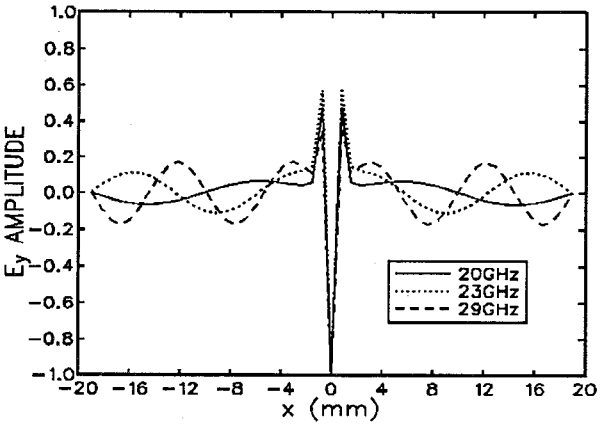

Fig. 5 Field plots for CBCPW mode demonstrating field spreading.

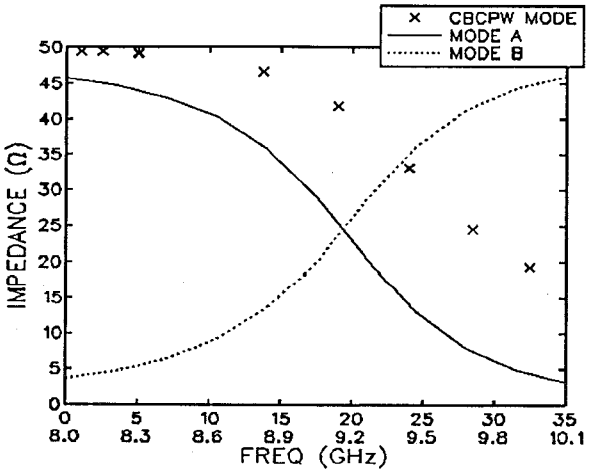

Fig. 6 Characteristic impedance plots for modes indicated in Fig. 2. MODES A, B refer to lower frequency range (8-10.1 GHz).

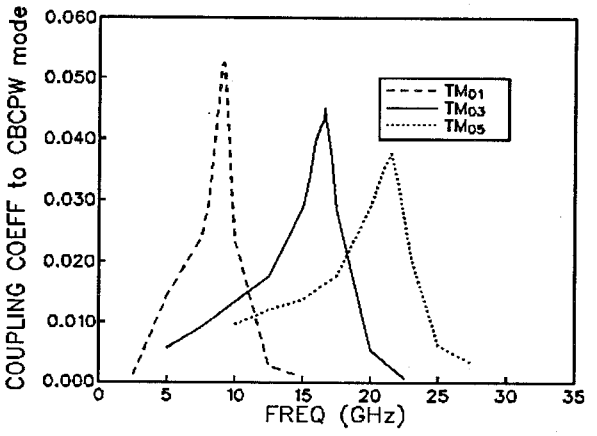

Fig. 7 Calculated coupling coefficient of waveguide modes to CBCPW mode.

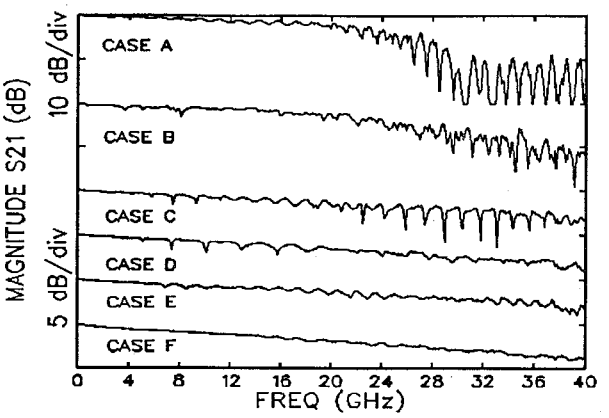

Fig. 8 Experimental data of approximate 50 Ω CBCPW MIC through lines. CASE A is the text numerical example for L=38 mm, CASE B (same as CASE A, L=25.4 mm), CASE C (ε_{r2}=2.33 h_2=0.71 mm, ε_{r1}=10.8 h_1=0.635 mm, W=2S=0.635 mm, L=38 mm, 2b=20 mm), CASE D (same as CASE C, L=25.4 mm), CASE E (same as CASE C except absorber at connector housing width at z=0, *L*), CASE F (same as CASE E, h_1=0.254 mm). CASES A, B refer to 10 dB/div scale. All examples referenced to 0 dB.